ASSESSING THE VOLCANIC HISTORY OF THE PRINZ-HARBINGER REGION OF THE MOON USING RADAR AND SPECTROSCOPY. Erica R. Jawin[1] and James W. Head[1], [1]Dept. Earth, Environ. & Planet. Sci., Brown University, Providence, RI USA (Erica_Jawin@brown.edu).

Introduction: The Prinz-Harbinger region of the Moon contains a large diversity of volcanic features including sinuous rilles, pyroclastics, and a broad topographic rise interpreted to represent a medium-scale shield volcano (*1*, *2*). This region, ~100 km east of the Aristarchus Plateau, is bound by Prinz crater to the southwest and Montes Harbinger to the northeast. The proximity to the Aristarchus Plateau and similarly high density of volcanic features make this region an important area to assess the relationship between explosive and effusive volcanism on the Moon. Explosive volcanic activity is indicated by the presence of pyroclastic material in the region, while effusive volcanism is indicated by the presence of sinuous rilles and the "circular rise" (*2*). However, the detailed relationship between effusive and explosive volcanism has not been adequately addressed in this region.

In this work, we used a combination of remotely sensed data, including Earth-based radar data and VNIR spectroscopy, to assess the physical and mineralogical nature of the Prinz-Harbinger region.

Methods: Analyses were performed using a combination of remotely sensed data, including radar data from the Arecibo Observatory at S- and P-band wavelengths (12.6 and 70 cm, respectively). Radar data are reported in terms of depolarized radar echoes, or same-sense circular polarization (SC), as well as circular polarization ratio (CPR) data. Spectral data from the Moon Mineralogy Mapper (M^3) were utilized from the OP1B optical period.

Observations: *Radar observations:* P-band SC radar data show that the entire Prinz-Harbinger region exhibits lower radar returns than the surrounding mare (Fig 1 top). The distribution of the low-backscatter area is of the same extent as the circular rise identified in (*2*); this unit is embayed by mare basalts that have higher SC radar returns.

On the center of the circular rise is a rimless depression that has anomalously high radar echoes relative to the rest of the region (red arrow, Fig 1 top). This higher scattering region is reflected in both S- and P-band radar data (Fig 1). In visible and detrended topography data (*2*), a small channel can be seen emanating from the west of this depression.

S-band SC data show a region on the circular rise of higher radar backscatter, specifically emanating from the rimless depression and extending to the north (red outline, Fig 1 bottom). This region has relatively higher radar echo strength than the surrounding region, and comparable strength to that of the surrounding mare.

CPR data also show a pronounced decrease on the circular rise relative to the surrounding mare in both S- and P-bands. Average S-band CPR values on the circular rise are ~0.36, while average P-band CPR values are lower, ~0.25.

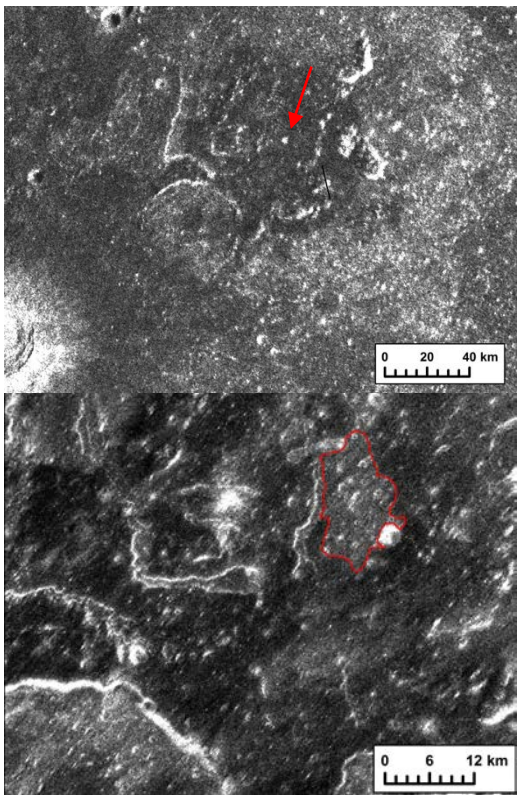

Fig 1. Top: P-band SC data. Dark region indicates the pyroclastic deposit due to low radar backscattering. Red arrow notes location of high backscatter indicating a potential volcanic vent. Bottom: S-band SC data. Red outline notes a region of higher backscatter, potentially indicating a buried lava flow.

Spectral observations: VNIR spectra were sampled at various locations in the region (Fig 2). These spectra show that in general, the surface of the circular rise is spectrally homogeneous, including the volcanic crater Ivan, the northern surface of the circular rise, and the eastern portion of the circular rise adjacent to the Montes Harbinger. These regions all contain very shallow absorption bands and low albedo. Absorptions are present at ~1000 nm, with shallower features at ~1250-1300 nm, and broad absorptions around 2000-2100 nm. In comparison, spectra taken from within the volcanic crater Vera, and a crater in the surrounding mare to the northeast of

the circular rise, have much deeper absorption features. The Vera spectrum has a high albedo relative to the other spectra, a broad 1 µm band and a 2 µm band centered at ~2000 nm. The mare spectrum has a similar 1 µm band shape and location, but a 2 µm band at longer wavelengths, ~2200 nm. In general, the Prinz-Harbinger region contains little spectral diversity on the surface of the circular rise, but spectral distinctions can be observed between the circular rise and the surrounding mare basalts.

Interpretations: The spectral and radar data support the previous observation that the Prinz-Harbinger region is mantled by pyroclastic material (*1*). CPR values of the Prinz-Harbinger region are consistent with pyroclastic mantling: S- and P-band CPR values of 0.36 and 0.25, respectively, are in very good agreement with CPR values from the Aristarchus pyroclastic deposit, 0.35 and 0.17 for S- and P-band, respectively, and also agree with previous radar analyses of lunar pyroclastic deposits and CPR values at different wavelengths (*3*-5). Spectral characteristics including shallow absorptions, red slopes, and low albedo also support the presence of pyroclastics.

The spectra of the Prinz-Harbinger surface lack traditional glass absorption bands as have been identified in other pyroclastic deposits (e.g., 6); however, glass-free pyroclastic deposits have been identified that resemble lunar pyroclastic deposits in physical and morphological characteristics, but do not contain spectral evidence of volcanic glass (7). The Prinz-Harbinger deposit is therefore interpreted to be distinct from the nearby Aristarchus pyroclastic deposit, which is very glass-rich (*8*).

The rimless depression shows high radar backscatter, which could be due to a rougher surface and/or lack of pyroclastic mantling; LROC NAC images confirm that there is a high concentration of boulders inside the depression. The irregular shape of the depression, lack of a raised rim, and channel extending to the west, suggest this is not an impact crater. Rather, it could be the location of an eruptive vent. The higher S-band SC region emanating to the west and north from this depression (Fig 1) are interpreted to indicate a shallowly buried lava flow; similar buried flows have been identified using radar data on the Aristarchus plateau (9). This buried flow, as well as the channel extending to the west, suggest that this region hosted a long period of volcanic activity.

There are not obvious flow features apparent in visible images near the potential vent, and this region is not resolvable in the P-band radar data; this suggests that the flow is thin and shallowly buried, so as to be masked by the deeper penetration depth of P-band radar (~15 m probing depth of P-band, compared to ~3 m in S-band). In addition, the shorter S-band radar data are sensitive to the presence of smaller blocks (>2 cm), relative to the sensitivity of P-band (10 cm).

The widespread distribution of pyroclastic material in the region suggests it is a stratigraphically young unit; Explosive eruptions therefore were occurring in the latest stage of volcanism in the Prinz-Harbinger region, post-dating the effusive volcanism that formed the circular rise, and potentially sourced from the formation of the abundant stratigraphically young sinuous rilles in the region (*2*). The connection between sinuous rilles and gas-rich, explosive volcanism is also indicated by the presence of irregular mare patches (IMPs) within the sinuous rille Rima Prinz (10). However, the presence of a stratigraphically young effusive flow and volcanic vent in the central portion of the region, separate from the sinuous rilles, suggests that effusive volcanism also occurred for an extended period of time. The variety of volcanic eruptions within a spatially restricted area suggests either discrete mantle sources for eruptions, or a variable volatile content within a single magma source.

References: 1. Zisk *et al.*, *The moon*. 17, 59–99 (1977). 2. Jawin *et al.*, 48th LPSC, Abs. 1184 (2017). 3. Carter *et al.*, *JGR*. 114, E11004 (2009). 4. Campbell *et al.*, *JGR*. 114, E01001 (2009). 5. Jawin *et al.*, *JGR*. 119 (2014). 6. Jawin *et al.*, *JGR*. 120, 1310–1331 (2015). 7. Besse *et al.*, *JGR*, 119, 2 (2015). 8. Gaddis *et al.*, *Icarus*, 161, 262–280 (2003). 9. Campbell *et al.*, *Geology*. 36, 135–138 (2008). 10. Zhang *et al.*, *Icarus*, in press (2017).

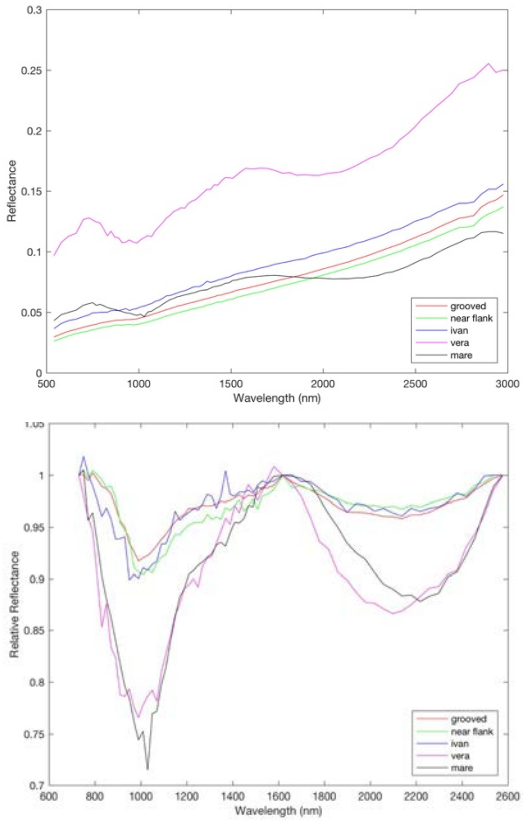

Fig 2. Top: Spectra of the Prinz-Harbinger region at various locations. Bottom: Continuum-removed spectra.